12-26-2021

Heterologous phasin expression in *Rhodopseudomonas palustris* CGA009 for bioplastic production from lignocellulosic biomass

Brandi Brown

Cheryl Immethun

Adil Alsiyabi

Dianna Long

Mark Wilkins

See next page for additional authors

Authors
Brandi Brown, Cheryl Immethun, Adil Alsiyabi, Dianna Long, Mark Wilkins, and Rajib Saha

Metabolic Engineering Communications 14 (2022) e00191

Contents lists available at ScienceDirect

Metabolic Engineering Communications

journal homepage: www.elsevier.com/locate/mec

Heterologous phasin expression in *Rhodopseudomonas palustris* CGA009 for bioplastic production from lignocellulosic biomass

Brandi Brown [a], Cheryl Immethun [b], Adil Alsiyabi [b], Dianna Long [b], Mark Wilkins [a,c,d], Rajib Saha [b,*]

[a] Department of Biological Systems Engineering, University of Nebraska-Lincoln, Lincoln, NE, 68583, USA
[b] Department of Chemical and Biomolecular Engineering, University of Nebraska-Lincoln, Lincoln, NE, 68588, USA
[c] Industrial Agricultural Products Center, University of Nebraska-Lincoln, Lincoln, NE, 68583, USA
[d] Department of Food Science and Technology, University of Nebraska-Lincoln, Lincoln, NE, 68588, USA

ARTICLE INFO

Keywords:
Phasin
Bioplastic
Lignocellulosic
Lignin
Rhodopseudomonas palustris
Polyhydroxybutyrate

ABSTRACT

Rhodopseudomonas palustris CGA009 is a metabolically robust microbe that can utilize lignin breakdown products to produce polyhydroxyalkanoates (PHAs), biopolymers with the potential to replace conventional plastics. Our recent efforts suggest PHA granule formation is a limiting factor for maximum production of the bioplastic poly (3-hydroxybutyrate-co-3-hydroxyvalerate) (PHBV) by *R. palustris*. The Phap1 phasin (*phaP1*) from the PHB-producing model bacterium *Cupriavidus necator* H16 was expressed in *R. palustris* with the aim of over-producing PHBV from the lignin breakdown product *p*-coumarate by fostering smaller and more abundant granules. Expression of *phaP1* yielded PHBV production from *R. palustris* aerobically (0.7 g/L), which does not occur in the wild-type strain, and led to a significantly higher PHBV titer than wild-type anaerobic production (0.41 g/L). The 3HV fractions were also significantly increased under both anaerobic and aerobic conditions, which boosts thermomechanical properties and potential for application. Thus, heterologous phasin expression in *R. palustris* provides flexibility for industrial processing and could foster compositional changes in copolymers with better thermomechanical properties compared to PHB alone.

1. Introduction

Polyhydroxyalkanoates (PHAs) are biopolymers produced by bacteria that have the potential to replace conventional plastics due to their similar thermomechanical properties, biodegradability, and biocompatibility (Li et al., 2016; Muneer et al., 2020; Sabbagh and Muhamad, 2017). Due to these characteristics, PHAs have been applied in a wide variety of applications including therapeutics, packaging, and environmental rehabilitation (Bello-Gil et al., 2018; Draper and Rehm, 2012; Hungund et al., 2018; Parlane et al., 2017). Bacteria typically produce PHAs in response to stressful conditions, such as unbalanced growth, and store the granules inside the cell as a means of carbon and redox balance (Koller, 2020). The most commonly produced PHA by bacteria is called poly-3-hydroxybutyrate (PHB) and is thus the most extensively studied. However, market acceptance of PHAs is limited by their relatively high production costs compared to conventional plastics (Aramvash et al., 2018). PHA costs depend mainly on the carbon source, fermentation technology, and extraction processes (Chen et al., 2020; Medeiros et al., 2020). Approximately half of the production cost for PHAs derives from the carbon source (Raza et al., 2018). Thus, engineering a microbe for PHA production from cheaper and renewable carbon sources is necessary to promote the valorization of PHAs.

Lignocellulosic biomass is considered to be the most economic carbon source in the world and is thus an ideal candidate for cheaper production of bioplastics (Ponnusamy et al., 2019; Qian, 2013). Using inexpensive and renewable carbon sources for bioplastic production that do not compete with food production, such as lignocellulosic biowaste, could significantly reduce the costs of bioplastics while simultaneously closing the carbon loop. Lignin is a heterogeneous network of cross-linked aromatics that accounts for nearly 30% of the organic carbon in plant biomass (Ponnusamy et al., 2019). The production of biopolymers from lignin is arguably one of the most promising routes for boosting the valorization of lignin (Rajesh Banu et al., 2019). Yet, one of the major challenges for valorizing lignin is developing an efficient bioconversion process to create value-added bioproducts from lignin breakdown products (LBPs), such as monolignols and hydroxycinnamic acids. Unfortunately, most microorganisms that can produce

* Corresponding author.
E-mail address: rsaha2@unl.edu (R. Saha).

https://doi.org/10.1016/j.mec.2021.e00191
Received 1 September 2021; Received in revised form 17 December 2021; Accepted 26 December 2021
Available online 29 December 2021

Abbreviations

3-Hydroxybutyrate (3HB)
3-Hydroxyvalerate (3HV)
Gas chromatography-mass spectrometry (GC-MS)
Granule-associated proteins (GAPs)
Lignin breakdown products (LBPs)
Polyhydroxyalkanoates (PHAs)
Polyhydroxybutyrate (PHB)
Poly(3-hydroxybutyrate-co-3-hydroxyvalerate) (PHBV)
Transmission Electron Microscopy (TEM)

high-valued bioproducts cannot metabolize LBPs and are even inhibited by them. Thus, employing synthetic biology techniques and metabolic engineering to over-produce PHAs from microbes capable of catabolizing this cheaper and renewable carbon source is ideal. Efforts in synthetic biology and metabolic engineering offer opportunities for overproduction of PHAs (Koller, 2017; Raza et al., 2018), but there is still a need to engineer a microbe for more cost-competitive production of PHAs from lignocellulosic biomass.

Bacteria that produce PHAs utilize an ensemble of granule-associated proteins (GAPs) that help balance metabolic tradeoffs in cell growth, PHA production, and other functions. This system of GAPs includes polymerases, depolymerases, synthases (PhaC), phasin regulators (PhaR), and phasins (Choi et al., 2020; Pillai et al., 2019). Of these proteins, phasins are a fascinating class of small-molecular weight proteins that perform multiple functions for the cell. Phasins are employed by all PHA-producing bacteria and are the dominant protein surrounding the PHA granules (Mezzina and Pettinari, 2016). Although originally thought to simply create a boundary layer between the granule and the cytoplasm, phasins have been revealed to perform a number of additional functions such as controlling the size, shape, and abundance of granules in the cell (Sharma et al., 2016), activating PHA depolymerization (Chen and Zhang, 2018), fostering granule segregation (Maestro et al., 2013), modulating expression of PHA synthases (Qi et al., 2000; Ushimaru et al., 2014), fostering localization of granules (Pfeiffer and Jendrossek, 2012), altering the composition of PHAs (Kawashima et al., 2015), and performing chaperone-like activities that contribute to cell fitness (Almeida et al., 2011). Interestingly, a single bacterium can

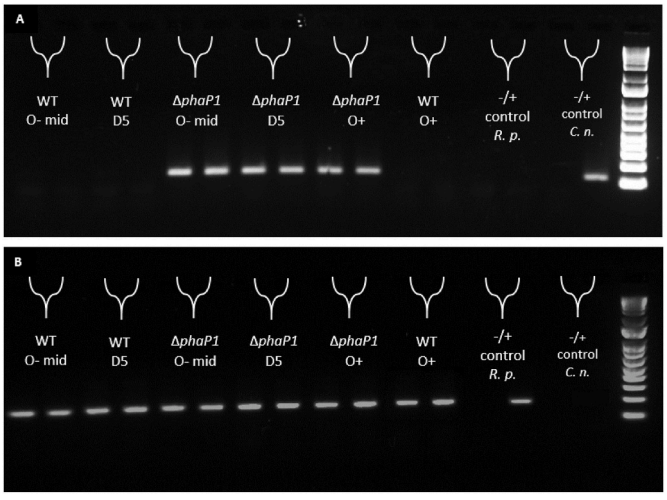

Fig. 1. Gene expression in the wild type (WT) vs. *phaP1* strains for (A) *phaP1* and (B) *16S rRNA* for aerobic (O+) and anaerobic (O-) conditions. The negative and positive controls represent water vs. gDNA for either *R. palustris* or *C. necator*.

employ multiple phasins that perform differing functions in the cells or are homologs of a dominant phasin that controls PHA production in the cell. For example, *Cupriavidus necator* H16 (formerly known as *Ralstonia eutropha*) is a model bacterium for PHB production that has arguably had the most characterization of its phasins, with seven different phasins discovered in the microbe (Sharma et al., 2016). Although *C. necator* employs seven different phasins for PHB metabolism, Phasin 1 (PhaP1) is the dominant phasin impacting PHB production. Kuchta et al. (2007) performed a detailed analysis of PhaP1 and three of its homologs (PhaP2-4) via engineering phasin-negative mutants to examine the *in vivo* functions of phasins in *C. necator*. PhaP1 was identified as the major phasin to control PHB production, and the absence of other phasins did not yield significant impact on PHB synthesis or accumulation compared to wild type. Phasins 2–4 are homologs of Phasin 1 that are synthesized in much smaller amounts under permissive conditions, while Phasins 5–7 are not homologs and still require further characterization (Maestro and Sanz, 2017; Pötter et al., 2004; Pfeiffer and Jendrossek, 2012). As the dominant phasin employed by *C. necator*, PhaP1 has been shown to control the size and number of granules in the cell, impact PHB accumulation and degradation rates, foster localization of granules, and manipulate the copolymer compositions of PHAs (Kawashima et al., 2015; Kuchta et al., 2007; Pfeiffer and Jendrossek, 2012; Pötter et al., 2004; Sharma et al., 2016). Although it is still unclear why *C. necator* employs multiple and redundant phasins for PHB metabolism, identifying the major phasin that is involved in controlling PHB production provides a platform for developing heterologous systems for PHA overproduction in other microbes.

Rhodopseudomonas palustris CGA009 (hereafter *R. palustris*) is a purple non-sulfur bacterium capable of fixing CO_2 and nitrogen or breaking down organic compounds for its carbon and nitrogen requirements, yielding several high-value product streams like bioplastics and biohydrogen (Brown et al., 2020; Larimer et al., 2004; McKinlay et al., 2014). This makes *R. palustris* an excellent candidate for engineering towards industrial production. As a metabolically robust bacterium, *R. palustris*' genome includes pathways for three of the four known microbial lignin degradation strategies, incorporating both aerobic and anaerobic photosynthetic catabolism (Larimer et al., 2004). Thus, *R. palustris* can break down numerous aromatic compounds derived from lignin while also potentially accomplishing complete degradation of these compounds to intermediates in the citric acid cycle that are important building blocks for bioplastic development. Our recent works show that *R. palustris* can utilize the major LBPs *p*-coumarate and coniferyl alcohol to produce bioplastics (Alsiyabi et al., 2021; Brown et al., 2020). We also revealed that *R. palustris* can create a copolymer of PHB called poly (3-hydroxybutyrate-co-3-hydroxyvalerate) (PHBV), which is a copolymer of the 3-hydroxybutyrate (3HB) and 3-hydroxyvalerate (3HV) monomers that has more ideal thermomechanical properties compared to PHB alone (Li et al., 2016).

In this study, *phaP1* from *C. necator* H16 was expressed in *R. palustris* with the aim of overproducing PHAs from lignocellulosic sources. *R. palustris'* ability to produce PHBV from lignocellulosic biomass renders it an ideal candidate for engineering toward industrial PHA production from lignin. However, our recent efforts also revealed that granule formation may be a limiting factor for maximum PHBV production due to one large PHBV granule formed inside the cells (Alsiyabi et al., 2021). Thus, heterologous expression of *phap1* was implemented in *R. palustris* with the aim of overproducing PHBV from lignocellulosic biomass by fostering smaller and more abundant granules to utilize more of the intracellular space.

2. Materials and methods

2.1. Growth curves and PHBV production

R. palustris seed culture was grown on photosynthetic media (PM) supplemented with 20 mM sodium acetate to an OD_{660} of approximately

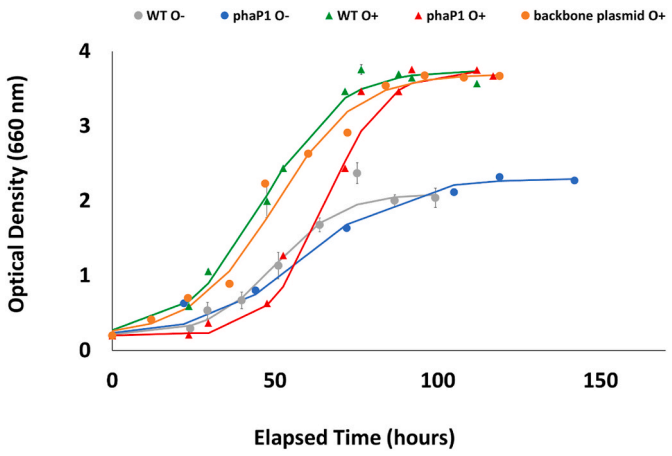

Fig. 2. Growth comparison between the wild type (WT), *phap1*, and backbone plasmid strains. The backbone plasmid strain was grown and tested aerobically only to serve as a control for assessing PHBV production. Data points are averages of biological triplicates, and errors bars are the calculated standard deviation. All conditions were grown on 1 mM *p*-coumarate and 10 mM sodium bicarbonate.

0.5 as described previously (Brown et al., 2020). All conditions employing the *phaP1* and backbone plasmid (pBBR1MCS-2) strains were supplemented with kanamycin (300 μg/mL). Cultures were diluted to an OD_{660} of 0.2 in fresh PM supplemented with 1 mM *p*-coumarate and 10 mM sodium bicarbonate as the carbon courses in anaerobic and aerobic conditions. Anaerobic cultures were grown in sealed 14 mL Falcon™ round-bottom polystyrene tubes at 30 °C with 100 μE white light and continuous shaking at 275 rpm. Falcon™ tubes were sealed to the second position via the secure snap-cap to provide a secure, positive seal. Oxygen depletion is assumed for anaerobic cultures after the tubes are sealed. Aerobic cultures were grown in the dark using 250 mL flasks with no more than 50 mL of total culture volume in each flask, at 30 °C, and with continuous shaking at 275 rpm. Growth data were fitted to a modified logarithmic growth model as described previously (Brown et al., 2020). For anaerobic conditions, cultures were nitrogen starved at mid-exponential growth by resuspending the cell pellet in fresh PM without ammonium sulfate as a nitrogen source that was supplemented with 1 mM *p*-coumarate and 10 mM sodium bicarbonate. Anaerobic samples were harvested for PHBV extraction upon nitrogen starvation (day 0) and on each day after nitrogen starvation for 11 days. For aerobic conditions, samples were prepared for PHBV analysis at each time point designated in Fig. 3B.

2.2. PHBV quantification via gas chromatography-mass spectrometry (GC-MS)

PHBV extraction and quantification was conducted as described previously (Brown et al., 2020). All harvested samples were washed twice with 1x phosphate buffered saline (PBS), stored as cell pellets in −80 °C until further processing, and extracted via acidic methanolysis. PHBV was quantified with conventional GC-MS as described (Brown et al., 2020), using serial dilutions of sodium 3-hydroxybutyrate or (−)-methyl (R)-3-hydroxyvalerate (Sigma-Aldrich™) as external standards.

2.3. Isolation, amplification, and manipulation of DNA

C. necator was grown on rich media (17.5 g/L nutrient broth, 7.5 g/L yeast extract, 5 g/L $(NH_4)_2SO_4$) to an OD_{600} of approximately 1.0 (Nangle et al., 2020). *R. palustris* was grown as described in Section 2.1. Chromosomal DNA was extracted using a *Quick*-DNA Fungal/Bacterial kit per manufacturer instructions (Zymo Research). The plasmid was constructed using the Hot Fusion assembly method (Fu et al., 2014). The oligonucleotides and plasmids are summarized in Table 1. The oligonucleotides were purchased from Eurofins Genomics. Enzymes were purchased from Thermo Fisher Scientific.

2.4. Strain construction

The PSSBIO32-tonB-*phaP1* plasmid was constructed in NEB® 10-beta competent *E. coli*. *E. coli* was grown overnight, diluted to 0.025%, grown for 2 h, and washed twice with autoclaved H_2O (Tu et al., 2016). The washed cells were transformed with the Hot Fusion products via electroporation. The electroporated cells were allowed to rest at 30 °C for 1–1.5 h in Luria Broth (LB) (Miller, AMRESCO) at 30 °C and 250 rpm in 14 mL BD Falcon™ round-bottom tubes without antibiotics, and subsequently plated onto LB plates supplemented with kanamycin (30

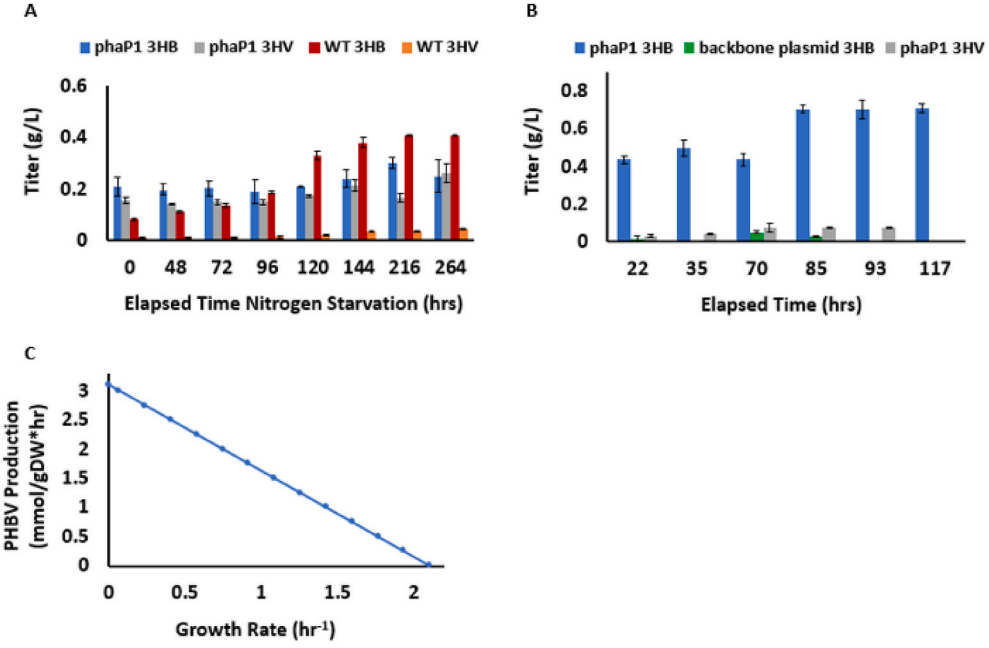

Fig. 3. PHBV monomer production in (A) anaerobic conditions from the wild type (WT) and *phaP1* strains, (B) aerobic conditions from the *phaP1* and backbone plasmid (pBBR1MCS-2) strains, and (C) Trade-off plot comparing the *phaP1* strains's growth rate with PHBV production strain under aerobic conditions generated through the application of the *iRpa940* genome-scale metabolic model. Wild type *R. palustris* yielded no measurable PHBV monomer production under aerobic conditions and is thus not shown on the graph in (B). The backbone plasmid was used as a control under aerobic conditions to decipher if the stress of plasmid maintenance alone fostered PHBV production since the wild type strain yielded no production aerobically. Data points represent biological triplicates, and error bars are the calculated standard deviation. All conditions were grown on 1 mM *p*-coumarate and 10 mM sodium bicarbonate.

Table 1
Bacterial strains, plasmids, and oligonucleotides used in this study.

Strain, plasmid, or oligonucleotide	Description	Source or reference
Strains		
Rhodopseudomonas palustris CGA009	Wild-type	*Rhodopseudomonas palustris* (Molisch) van Niel BAA-98™
phaP1	*R. palustris* expressing the PhaP1 phasin from *C. necator* H16	This study
Cupriavidus necator H16	Wild-type	DSM 428
Escherichia coli DH10B	NEB 10-beta Competent *E. coli* is a derivative of the popular DH10B. It is T1 phage resistant and endonuclease I (endA1) deficient for high-quality plasmid preparations.	New England Biolabs®, Inc.
Plasmids		
pBBR1MCS-2	Empty Backbone; Mobilisable shuttle and expression vector	Kovach et al. (1995)
pBBR1 ori; kan^R; P$_{Lac}$-phaP1		Kovach et al. (1995)
Oligonucleotides for plasmid building		
H16 (F)	GAGTTTGGATCCTTAAGCACTCAGGCAGCCGTCGTCTTCTTTG	*C. necator* gDNA
H16 (R)	GAATTGTGAGCGGATAACAACTTAATTTGCTTGACCTTGAAGTTCACCAC	
rrnbTerm (R)	GTGCTTAAGGATCCAAACTCGAG	PSSBIO32-tonB, a derivative of pBBR1MCS-2
Lac01 (F)	TTGTTATCCGCTCACAATTCCACAC	
Sequencing Lac (F)	GAACGAAGTCTTGACGACCTG	PSSBIO32-tonB-*phaP1*, this study
Sequencing Lac (R)	GTTTGTGTCCACGACAGGTTTC	
Sequencing rrnb (F)	GCACCTCGCTAACGGATTCAC	
Sequencing rrnb (R)	CACCAAGGCGTTTGAAGGCGTC	
Oligonucleotides for RT-PCR		
16SrRNA (F)	CAGGACCGGTCGCAGAGACG	*R. palustris* cDNA
16SrRNA (R)	GACGTCATCCCCACCTTCCTC	
Phap1 (F)	CTGACCACCAAGGCGTTTGAAGG	*R. palustris* cDNA
Phap1 (R)	CAGCAGTTCCTGTGCGTCCTTG	

μg/mL). Colonies were selected and cultures were frozen as 15% glycerol stock at −80 °C until further processing. Fresh culture was subjected to the Invitrogen™ PureLink™ Quick Plasmid Miniprep kit (ThermoFisher) to remove the plasmid per manufacturer's instructions. PCR using designed sequencing oligonucleotides was conducted with the plasmids, and gel electrophoresis was used to check the amplicon size. If the amplicon was the expected size, the reaction was purified with the Invitrogen™ PureLink™ Quick PCR Purification Kit (ThermoFisher), and submitted to Eurofins Genomics for sequencing.

Sequence-verified plasmids were transformed into *R. palustris* following the same washing and electroporation steps. The transformed cells rested in Van Niel's Yeast Media (ATCC Medium 112) and were plated 24 h later on Van Niel's Yeast Agar supplemented with kanamycin (300 μg/mL). Colonies were then streaked onto a new plate to supplement growth. Cells from this plate were lysed in water at 100 °C for 25 min. PCR with the designed sequencing oligonucleotides was conducted again, followed by gel electrophoresis to check the amplicon size, purification, and submission for sequencing.

2.5. RT-PCR reactions

To validate expression of *phaP1*, RT-PCR was conducted for the wild type and *phaP1* strains under aerobic and anaerobic conditions using the designed oligonucleotides outlined in Table 1. Cultures were grown to mid-exponential on *p*-coumarate as shown in Fig. 1, saved with RNALater® solution per manufacture instructions, and stored in −80 °C until further processing. RNA was extracted according to conventional chloroform-phenol extraction, and RNA samples were rid of DNA using the Invitrogen™ TURBO™ DNA-Free Kit (ThermoFisher). The RNA samples were purified using the Monarch® RNA Cleanup Kit (New England BioLabs). All samples were confirmed DNA-free due to a lack of a positive band via PCR with the RNA. Particular care was taken to assess degradation of the RNA samples via bleach gels (Aranda et al., 2012). Only RNA samples that did not yield a DNA band or show degradation via a bleach gel were converted into cDNA using a High-Capacity cDNA Reverse Transcription Kit per manufacture instructions (ThermoFisher). All cDNA samples were tested via RT-PCR using GoTaq® Green Master Mix (Promega) and the *16S rRNA* housekeeping gene (*RPA_RNA55*) to ensure a positive band. If the housekeeping gene did not reveal a positive band from RT-PCR using a certain cDNA sample, that sample was considered too low of quality for further analysis.

2.6. Transmission electron microscopy (TEM)

TEM was conducted to visualize granules inside the wild type and *phaP1* strains grown on *p*-coumarate in both aerobic and anaerobic conditions as described previously (Alsiyabi et al., 2021). Briefly, the samples were fixed in a 2% glutaraldehyde and 1.5% paraformaldehyde in 100 mM sodium cacodylate buffer and submitted to the Nebraska Center for Biotechnology Morrison Microscopy Core Research Facility at the University of Nebraska-Lincoln. The samples were processed further by washing in sodium cacodylate buffer three times, and post-fixing in 1% osmium tetroxide in deionized water at room temperature for 1 h. The samples were dehydrated through an ethanol series, embedded in Spurr medium, ultrathin section were cut using a Leica UC7 ultramicrotome, and the sections were stained with 1% uranyl acid and 1% lead citrate. Images were collected using a Hitachi H7500 TEM and taken without selection or bias.

2.7. Metabolic modeling

The trade-off plot between PHB and biomass production for the *phaP1* strain under aerobic conditions was generated by simulating (via flux balance analysis) aerobic growth on *p*-coumarate (Orth et al., 2010) using *R. palustris'* genome-scale metabolic model *iRpa940* (Alsiyabi et al., 2019, 2021). The maximal PHB and biomass generation rates were first determined by maximizing their respective reactions in the model. Next, biomass production was maximized while PHB production rate was set to increasing values between zero and maximal production. The maximum rate of carbon fixation was assumed to be equal to the rate in anaerobic growth (Alsiyabi et al., 2021). Furthermore, arbitrary uptake rates were set for *p*-coumarate and oxygen since the actual uptake rates are not known. However, the general observed trend in the trade-off plot should remain the same.

2.8. Statistical methods

Data points for growth curves and GC-MS data represent the averages

of biological triplicates, and error bars are the calculated standard deviation from raw data based on the population. Independent, two-tailed *t* tests were used to calculate statistical significance at a 95% confidence interval ($\alpha = 0.05$), and the *p* value is listed where appropriate.

3. Results and discussion

Our recent efforts suggested granule formation is a limiting factor for maximum production of PHBV by *R. palustris* due to one large granule predominately being formed inside the cells (Alsiyabi et al., 2021). PhaP1 leads to smaller and more abundant PHB granules in *C. necator*, and it was hypothesized that expression of *phaP1* would increase overall PHBV monomer titers from *R. palustris*. Thus, *phaP1* was expressed in *R. palustris* with the aim of overproducing PHBV from lignocellulosic sources by maximizing the use of intracellular space via producing smaller and more abundant granules.

3.1. Gene expression analysis for phaP1

Gene expression analysis was first conducted via RT-PCR to verify the expression of *phaP1* in the *phaP1* strain compared to the wild type strain. Fig. 1 depicts the expression bands for *phaP1* and *16S rRNA* in each condition. All conditions showed significant expression of the *16S rRNA* housekeeping gene. Furthermore, all conditions for the *phaP1* strain yielded expression of *phaP1*, whereas the wild type strain did not. In Fig. 1A, the positive and negative controls using *R. palustris* gDNA did not yield expression, which was to be expected since *phaP1* is naturally occurring in *C. necator*. In Fig. 1B, the controls for *16S rRNA* using *C. necator* gDNA did not yield expression since this occurs naturally in *R. palustris*.

3.2. Comparisons of growth and PHBV production

Analyses were conducted to assess the impacts on growth and production of PHBV monomers due to *phaP1* expression in *R. palustris*. First, we conducted growth comparison analyses for both aerobic and anaerobic environments to decipher if growth was impacted by expression of *phaP1*. Fig. 2 depicts the logarithmic growth curves of strains containing the backbone plasmid with *phaP1* inserted (*phaP1*), the backbone without *phaP1* (backbone plasmid), and the wild type (WT) strains. Under anaerobic conditions, there was no significant difference in maximum OD between the wild type and *phaP1* strains (*p* value = 0.395). There was also no significant difference in maximum OD between the wild type, *phaP1*, and backbone plasmid strains in aerobic conditions (*p* values > 0.05). Hence, expression of *phap1* did not yield significant changes in the maximum OD in neither anaerobic nor aerobic conditions. However, the *phaP1* strain yielded a slower growth rate in aerobic conditions compared to the wild type strain. Later, we discuss how we explore this further with the application of genome-scale metabolic modeling.

We then assessed changes in 3HV and 3HB production due to *phaP1* expression based on our hypothesis that *phaP1* expression would enhance production. Under anaerobic conditions, there was no statistical significance in maximum titers (i.e. 3HB + 3HV fractions) between the wild type and *phaP1* strains (*p* value = 0.137), but there was a significant difference in 3HV fractions between the strains (Fig. 3A). The *phaP1* strain generated a significantly higher 3HV fraction (0.25 g/L) compared to the wild type strain (0.04 g/L) under anaerobic conditions (*p* value = 0.00316). Expression of *phaP1* fostered 3HB and 3HB production from *R. palustris* aerobically, which does not occur in the wild type strain (Fig. 3B). Total production from the *phaP1* strain in aerobic conditions (0.7 g/L) was significantly higher than the maximum anaerobic titer (0.41 g/L) for the wild-type strain (*p* value $= 1.8 \times 10^{-7}$). The 3HV fraction generated aerobically from the *phaP1* strain (0.074 g/L) was also significantly higher than the wild type fraction (0.04 g/L) in anaerobic conditions (*p* value = 0.000126). The backbone plasmid strain was used as a control under aerobic conditions to decipher if *phaP1* expression yielded significantly higher 3HB and 3HV production compared to the backbone alone. The backbone plasmid strain produced a relatively small amount of 3HB (approximately 0.05 g/L maximum), which was merely 1/14 that of the production from the *phaP1* strain (0.7 g/L). Furthermore, the backbone plasmid strain did not yield any 3HV production, compared to 0.074 g/L generated from the *phaP1* strain. Statistical comparison of the 3HB (*p* value $= 1.243 \times 10^{-6}$) and 3HV (*p* value $= 5.402 \times 10^{-9}$) fractions produced from the backbone plasmid versus the *phaP1* strains is significant, which supports the hypothesis that aerobic PHBV production is significantly higher with *phaP1* expression compared to the backbone plasmid alone.

Once the growth and PHBV monomer fraction production analyses had been conducted, we wanted to further assess why the *phaP1* strain yielded a slower growth rate than wild type under aerobic conditions. It was hypothesized that the reduced growth rate could be due to tradeoffs between biomass and PHBV production. A genome-scale metabolic model of *R. palustris*, called *iRpa940*, was recently applied to compare tradeoffs in growth and PHB production from a variety of substrates including *p*-coumarate (Alsiyabi et al., 2021). Genome scale modeling synergizes results from the context of whole-cell metabolism, utilizing annotated breakdown pathways for the corresponding substrates. Since there was a lack of kinetic parameters and concentration ranges for PHBV production reactions in *R. palustris*, only tradeoffs corresponding to PHB were assessed previously. However, it is likely that the outcomes utilizing the model are very comparable between PHB and PHBV since the monomer products are produced by the same enzymes. Thus, this genome-scale metabolic model was employed here to assess the hypothesis that the *phaP1* strain had a reduced growth rate due to the new PHBV production compared to wild type *R. palustris* (Alsiyabi et al., 2019, 2021). A plot comparing PHB and biomass production for the *phaP1* strain under aerobic conditions was generating via flux balance analysis simulations with *iRpa940* utilizing *p*-coumarate as the substrate (Fig. 3C). As expected, the relationship between growth rate and PHBV production is linear and reflects a direct negative correlation. Thus, since the *phaP1* strain produced 3HB and 3HV under aerobic conditions compared to no production from the wild type strain, the *phaP1* strain had a lower growth rate to compensate for the production.

In summary, expression of *phaP1* yielded increased 3HV fractions under both anaerobic and aerobic conditions, and fostered PHBV monomer production aerobically compared to no measurable aerobic production by the wild type strain. Increased 3HV fractions are desirable since they create a bioplastic with increased tensile strength, impact strength, and flexibility that render it more applicable in a wider array of applications (Heinrich et al., 2015). Our recent efforts identified several key metabolic factors impacting PHB production by *R. palustris* under anaerobic conditions (utilizing the Calvin Benson Bassham cycle as an electron sink), including a significant thermodynamic bottleneck for the thiolase reaction (phaA) as well as a significant dependence of the reductase reaction (phaB) on the NADP(H) redox state in the cells (Alsiyabi et al., 2021). Moreover, we found that a very high acetyl-CoA/CoA ratio is required to render the thiolase reaction thermodynamically feasible, reductase (phaB) is linearly dependent on the NADPH/NADP ratio, and reductase will likely be rate-limiting regardless of metabolic conditions due to low catalytic efficiency (Alsiyabi et al., 2021). Increased production of 3HV is linked to increased propionyl-CoA pools, whereby β-ketothiolase conducts condensation of acetyl-coenzyme A (acetyl-CoA) and propionyl-CoA to form 3HV. Thus, it is hypothesized that expression of *phaP1* enables more efficient utilization of propionyl-CoA pools that fostered higher 3HV fractions (Mezzina et al., 2017). Due to the constitutive expression of PHB producing enzymes (Alsiyabi et al., 2021), the increased utilization efficiency of propionyl-CoA enabled by *phaP1* results in a higher rate of 3HV production. Under aerobic conditions, the presence of a highly electrophilic electron acceptor (oxygen) means that the wild type's propionyl-CoA utilization efficiency is not sufficient to shuttle electrons

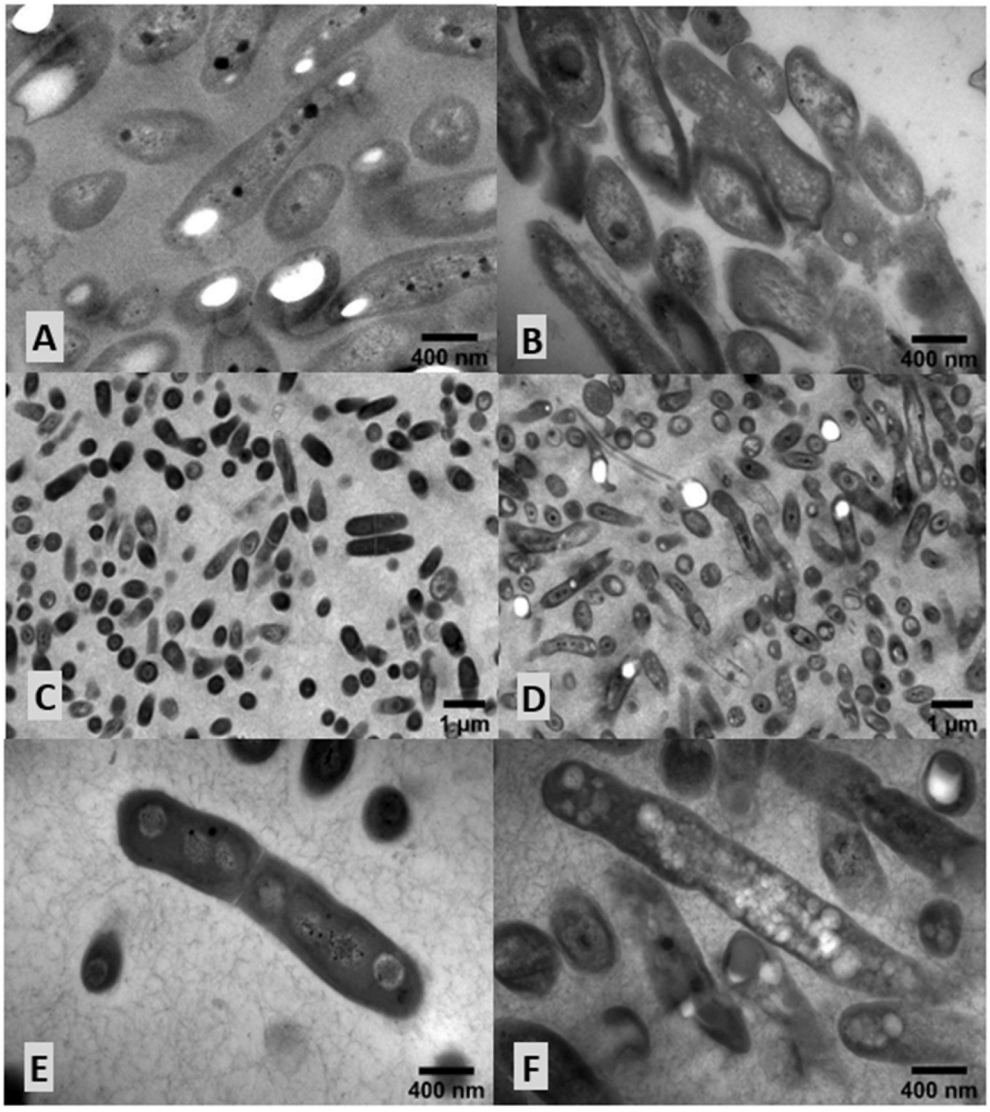

Fig. 4. TEM images of cells grown on *p*-coumarate for (A) wild type strain under anaerobic conditions, (B) *phaP1* strain under anaerobic conditions, (C) wild type strain under aerobic conditions, (D) *phaP1* strain under aerobic conditions, (E) wild type strain under aerobic conditions with higher magnification, and (F) *phaP1* strain under aerobic conditions with higher magnification. White inclusions inside the cells represent PHBV granules.

away from oxygen into 3HV, which explains why *phaP1* overexpression is required for 3HV production under such conditions. Although the expression of *phaP1* did not yield higher 3HB production compared to the wild type strain, the 3HV fraction was higher and ultimately yields a bioplastic with more desirable thermomechanical properties compared to PHB alone (Li et al., 2016). Hence, heterologous phasin expression in *R. palustris* could be a strategy for producing bioplastics that have improved market applicability via altering the monomer fractions of the polymer as shown in other organisms (Kawashima et al., 2015).

However, the mechanism for the fostered aerobic production due to *phaP1* expression is more elusive and will require more investigation in the future. Wild type *R. palustris* produces PHBV anaerobically via photoheterotrophy whereby it uses light as an energy source to pump protons out of the cell to maintain redox balance that allows ATP synthase to proceed (Larimer et al., 2004). Although *R. palustris* obtains energy from light under photoheterotrophy it must be supplemented with more carbon than carbon dioxide alone. We found in our recent efforts that the choice of substrate significantly impacts PHBV accumulation, and that utilizing more reduced substrates like *p*-coumarate fosters more PHBV accumulation compared to less reduced substrates like acetate (Alsiyabi et al., 2021). Under aerobic conditions (chemoheterotrophy), a proton motive force is built by releasing protons from the cell via an electron transport chain, and ATP synthases use protons to form ATP from ADP. In other words, glycolysis, β-oxidation of free fatty acids, and the TCA cycle generate reducing equivalents under aerobic conditions. Thus, there is not as much of a need to formulate PHBV under aerobic conditions due to the innate differences in redox balances for the metabolisms. Interestingly, expression of *phaP1* in *R. palustris* fostered PHBV production aerobically compared to no measurable PHBV production by the wild type strain. PhaP1 performs a large role in the stability and mobilization of PHB inclusions in *C. necator* in which a PhaP1-negative mutant renders PHB autodegradation, so this granule stability could be one mechanism that fostered aerobic production in *R. palustris* (Kuchta et al., 2007). Additionally, altering the surface to volume ratios of granules is one proposed indirect effect phasins have regarding interactions of phasins with PHB deploymerases. Since many granule-associated-proteins are constitutatively expressed in both *C. necator* and *R. palustris* (e.g. PHB synthases and deploymerases), changes in phasin expression has been shown to have a large impact on PHB production due to interactions with these proteins (Kuchta et al., 2007). Another plausible cause for the aerobic production due to the expression of *phaP1* is that PhaP1 is strictly regulated by PhAR

at the transcription level in *C. necator* in which PhaP1 production is based on the amount of PHB in cells and the presence of PhaC synthase, and heterogenous expression in *R. palustris* might not have this regulatory mechanism (Maestro and Sanz, 2017; Pötter et al., 2002; York et al., 2002). Thus, more effort is needed to identify the mechanisms behind PhaP1 in this heterogenous system with *R. palustris*, and in particular in aerobic environments. In the end, engineering the production of PHBV aerobically by *R. palustris* boosts the industrial production potential since it provides flexibility for industrial processing.

Ultimately, *R. palustris* is a very metabolically robust bacterium with the ability to convert sustainable feedstocks (e.g. lignin) into several value-added products (PHBV, hydrogen, n-butanol). This makes *R. palustris* an attractive candidate for engineering toward industrial production, and through this study we further enhance *R. palustris'* PHBV production via expression of *phaP1* (Phasin 1) from the model bacterium *C. necator*. There are several routes for further engineering this system, which include improving the 3HV fractions under aerobic conditions by assessing tradeoffs between the methyl citric acid cycle and the methylmalonyl-CoA pathways (Steinbüchel and Lütke-Eversloh, 2003), creating other synthetic systems that incorporate more of the PHB chassis from *C. necator* or other organisms, and also by further characterizing and engineering *R. palustris'* native PHBV production chassis (e.g. phasins employed by *R. palustris*). After exploring changes in gene expression, growth, and PHBV monomer production due to the expression of *phaP1*, we next conducted TEM to decipher if expression indeed fostered changes in granule formation in *R. palustris*.

3.3. Changes in PHBV granule formation

In addition to the gene expression, growth, and PHBV production analyses, TEM was conducted to test the hypothesis that expression of *phaP1* in *R. palustris* would boost PHBV production by fostering smaller and more abundant granules. Fig. 4 depicts the TEM images of wild type cells (in the left column) versus *phaP1* cells (in the right column). Fig. 4A and B of the wild type and *phaP1* cells respectively in anaerobic conditions shows a discrepancy from the large, single granule produced in the wild type cells compared to smaller, and more numerous granules in the *phaP1* cells. There are some variations in terms of brightness between the PHBV granules, which can be attributed to the small granules getting replaced by embedding medium easier than the larger ones as well as variations in section thickness (Wahl et al., 2012). Furthermore, expression of *phaP1* appears to alter the subcellular localization of the PHBV granules in *R. palustris*, which has been shown in *C. necator* as well (Wahl et al., 2012). The granules in the cells from the *phaP1* strain are more dispersed inside the cells rather than remaining primarily at the poles. There is also a clear discrepancy between images taken of cells grown under aerobic conditions (Fig. 4C–F). Wild type *R. palustris* grown aerobically did not yield any PHBV titer, which is reflected in the lack of granules inside the cells (Fig. 4C, E). Expression of *phaP1* fostered PHBV production aerobically, which is supported by the granule formation observed in Fig. 4D, F. Ultimately, TEM analysis supports the hypothesis that expression of *phaP1* would foster changes in granule formation inside the cells, which also likely contributes to the altered PHBV production capabilities in each condition.

4. Conclusions

In this study the Phap1 phasin from *C. necator* was expressed in *R. palustris* to overproduce PHBV by creating smaller and more abundant granules and optimizing the use of intracellular space. Expression of *phaP1* yielded PHBV production from *R. palustris* aerobically (0.7 g/L), which does not occur in wild type, and to a significantly higher titer compared to wild type anaerobic production (0.41 g/L). The 3HV fractions were also significantly increased under both anaerobic and aerobic conditions. Thus, heterologous phasin expression in *R. palustris* provides flexibility for industrial processing and fosters compositional changes in copolymers with better thermomechanical properties compared to PHB alone.

Author statement

Brandi Brown: Conceptualization, Methodology, Software, Formal Analysis, Investigation, Writing - Original Draft, Resources, Data Curation, Visualization. **Cheryl Immethun:** Conceptualization, Methodology, Formal Analysis, Resources, Supervision, Writing - Review & Editing. **Adil Alsiyabi:** Methodology, Software. **Dianna Long:** Conceptualization, Methodology, Software. **Mark Wilkins:** Resources, Funding acquisition, Supervision, Writing - Review & Editing. **Rajib Saha:** Resources, Funding acquisition, Supervision, Writing - Review & Editing.

Declaration of competing interest

The authors declare that they have no known competing financial interests or personal relationships that could have appeared to influence the work reported in this paper.

Acknowledgments

We gratefully acknowledge funding support from National Science Foundation (NSF) CAREER grant (25-1106-0039-001), Nebraska Center for Energy Science and Research grants (26-1217-0020-403 and 26-1217-0020-413), National Science Foundation (NSF) EPSCoR Center for Root and Rhizobiome Innovation grant (25-1215-0139-025), NSF MCB grant (25-1215-0175-001), and U.S. Department of Agriculture National Institute of Food and Agriculture (USDA-NIFA) Postdoctoral Fellowship (2019-67012-29632). We extend special thanks to Mark Kathol for sample collection at difficult times. Additionally, we extend thanks to Dr. You Zhou at the University of Nebraska-Lincoln Microscopy Core Facility for providing guidance for running the experiments. We are also thankful to Anjeza Erickson and Dr. Sibel Irmak at the Industrial Agricultural Products Center for providing support with GC-MS analysis. Finally, we would like to thank Dr. Taity Changa and Mark Kathol for assisting with plasmid building.

References

Almeida, de A., Catone, M.V., Rhodius, V.A., Gross, C.A., Pettinari, M.J., 2011. Unexpected stress-reducing effect of PhaP, a poly(3-hydroxybutyrate) granule-associated protein, in Escherichia coli. Appl. Environ. Microbiol. 77, 6622–6629. https://doi.org/10.1128/AEM.05469-11.

Alsiyabi, A., Immethun, C.M., Saha, R., 2019. Modeling the interplay between photosynthesis, CO2 fixation, and the quinone pool in a purple non-sulfur bacterium. Sci. Rep. https://doi.org/10.1038/s41598-019-49079-z.

Alsiyabi, A., Brown, B., Immethun, C., Wilkins, M., Saha, R., 2021. Synergistic experimental and computational approach identifies novel strategies for polyhydroxybutyrate overproduction. Metab. Eng. 68, 1–13. https://doi.org/10.1016/j.ymben.2021.08.008. ISSN 1096-7176.

Aramvash, A., Moazzeni Zavareh, F., Gholami Banadkuki, N., 2018. Comparison of different solvents for extraction of polyhydroxybutyrate from Cupriavidus necator. Eng. Life Sci. https://doi.org/10.1002/elsc.201700102.

Aranda, P.S., LaJoie, D.M., Jorcyk, C.L., 2012. Bleach gel: a simple agarose gel for analyzing RNA quality. Electrophoresis 33, 366–369. https://doi.org/10.1002/elps.201100335.

Rajesh Banu, J., Kavitha, S., Yukesh Kannah, R.v, Poornima Devi, T., Gunasekaran, M., Kim, S.-H., Kumar, G., 2019. A review on biopolymer production via lignin valorization. Bioresour. Technol. 290, 121790 https://doi.org/10.1016/j.biortech.2019.121790.

Bello-Gil, D., Roig-Molina, E., Fonseca, J., Sarmiento-Ferrández, M.D., Ferrándiz, M., Franco, E., Mira, E., Maestro, B., Sanz, J.M., 2018. An enzymatic system for decolorization of wastewater dyes using immobilized CueO laccase-like multicopper oxidase on poly-3-hydroxybutyrate. Microb. Biotechnol 11, 881–892. https://doi.org/10.1111/1751-7915.13287.

Brown, B., Immethun, C., Wilkins, M., Saha, R., 2020. Rhodopseudomonas palustris CGA009 polyhydroxybutyrate production from a lignin aromatic and quantification via flow cytometry. Bioresour. Technol. Rep. 11, 100474 https://doi.org/10.1016/j.biteb.2020.100474.

Chen, G.Q., Zhang, J., 2018. Microbial polyhydroxyalkanoates as medical implant biomaterials. Artif. Cells, Nanomed. Biotechnol. https://doi.org/10.1080/21691401.2017.1371185.

Chen, G.-Q., Chen, X.-Y., Wu, F.-Q., Chen, J.-C., 2020. Polyhydroxyalkanoates (PHA) toward cost competitiveness and functionality. Adv. Ind. Eng. Polym. Res. 3, 1–7. https://doi.org/10.1016/j.aiepr.2019.11.001.

Choi, S.Y., Rhie, M.N., Kim, H.T., Joo, J.C., Cho, I.J., Son, J., Jo, S.Y., Sohn, Y.J., Baritugo, K.A., Pyo, J., Lee, Y., Lee, S.Y., Park, S.J., 2020. Metabolic engineering for the synthesis of polyesters: a 100-year journey from polyhydroxyalkanoates to non-natural microbial polyesters. Metab. Eng. https://doi.org/10.1016/j.ymben.2019.05.009.

Draper, J.L., Rehm, B.H., 2012. Engineering bacteria to manufacture functionalized polyester beads. Bioengineered. https://doi.org/10.4161/bbug.19567.

Fu, C., Donovan, W.P., Shikapwashya-Hasser, O., Ye, X., Cole, R.H., 2014. Hot Fusion: an efficient method to clone multiple DNA fragments as well as inverted repeats without ligase. PLoS One 9, e115318. https://doi.org/10.1371/journal.pone.0115318.

Heinrich, D., Raberg, M., Steinbüchel, A., 2015. Synthesis of poly(3-hydroxybutyrate-co-3-hydroxyvalerate) from unrelated carbon sources in engineered Rhodospirillum rubrum. FEMS Microbiol. Lett. 362 https://doi.org/10.1093/femsle/fnv038.

Hungund, B.S., Umloti, S.G., Upadhyaya, K.P., Manjanna, J., Yallappa, S., Ayachit, N.H., 2018. Development and characterization of polyhydroxybutyrate biocomposites and their application in the removal of heavy metals. Mater. Today Proc. 5 https://doi.org/10.1016/j.matpr.2018.06.495.

Kawashima, Y., Orita, I., Nakamura, S., Fukui, T., 2015. Compositional regulation of poly (3-hydroxybutyrate-co-3-hydroxyhexanoate) by replacement of granule-associated protein in Ralstonia eutropha. Microb. Cell Factories 14 (187). https://doi.org/10.1186/s12934-015-0380-8.

Koller, M., 2017. Advances in polyhydroxyalkanoate (PHA) production. Bioengineering. https://doi.org/10.3390/bioengineering4040088.

Koller, M., 2020. Advances in polyhydroxyalkanoate (PHA) production, volume 2. Bioengineering. https://doi.org/10.3390/bioengineering7010024.

Kovach, M.E., Elzer, P.H., Hill, D.S., Robertson, G.T., Farris, M.A., Roop 2nd, R.M., Peterson, K.M., 1995. Four new derivatives of the broad-host-range cloning vector pBBR1MCS, carrying different antibiotic-resistance cassettes. Gene 166, 175–176. https://doi.org/10.1016/0378-1119(95)00584-1.

Kuchta, K., Chi, L., Fuchs, H., Pötter, M., Steinbüchel, A., 2007. Studies on the influence of phasins on accumulation and degradation of PHB and nanostructure of PHB granules in ralstonia eutropha H16. Biomacromolecules 8, 657–662. https://doi.org/10.1021/bm060912e.

Larimer, F.W., Chain, P., Hauser, L., Lamerdin, J., Malfatti, S., Do, L., Land, M.L., Pelletier, D.A., Beatty, J.T., Lang, A.S., Tabita, F.R., Gibson, J.L., Hanson, T.E., Bobst, C., Torres Y Torres, J.L., Peres, C., Harrison, F.H., Gibson, J., Harwood, C.S., 2004. Complete genome sequence of the metabolically versatile photosynthetic bacterium Rhodopseudomonas palustris. Nat. Biotechnol. https://doi.org/10.1038/nbt923.

Li, Z., Yang, J., Loh, X.J., 2016. Polyhydroxyalkanoates: opening doors for a sustainable future. NPG Asia Mater. https://doi.org/10.1038/am.2016.48.

Maestro, B., Sanz, J.M., 2017. Polyhydroxyalkanoate-associated phasins as phylogenetically heterogeneous, multipurpose proteins. Microbial Biotechnol. 10, 1323–1337. https://doi.org/10.1111/1751-7915.12718.

Maestro, B., Galán, B., Alfonso, C., Rivas, G., Prieto, M.A., Sanz, J.M., 2013. A new family of intrinsically disordered proteins: structural characterization of the major phasin PhaF from Pseudomonas putida KT2440. PLoS One 8. https://doi.org/10.1371/journal.pone.0056904.

McKinlay, J.B., Oda, Y., Ruhl, M., Posto, A.L., Sauer, U., Harwood, C.S., 2014. Non-growing rhodopseudomonas palustris increases the hydrogen gas yield from acetate by shifting from the glyoxylate shunt to the tricarboxylic acid cycle. J. Biol. Chem. https://doi.org/10.1074/jbc.M113.527515.

Medeiros, Garcia, Alcântara, J., Distante, F., Storti, G., Moscatelli, D., Morbidelli, M., Sponchioni, M., 2020. Current trends in the production of biodegradable bioplastics: the case of polyhydroxyalkanoates. Biotechnol. Adv. https://doi.org/10.1016/j.biotechadv.2020.107582.

Mezzina, M.P., Pettinari, M.J., 2016. Phasins, multifaceted polyhydroxyalkanoate granule-associated proteins. Appl. Environ. Microbiol. 82 https://doi.org/10.1128/AEM.01161-16, 5060 LP – 5067.

Mezzina, M.P., Álvarez, D.S., Egoburo, D.E., Peña, R.D., Nikel, P.I., Pettinari, M.J., 2017. A new player in the biorefineries field: phasin PhaP enhances tolerance to solvents and boosts ethanol and 1,3-propanediol synthesis in Escherichia coli. Appl. Environ. Microbiol. 83 https://doi.org/10.1128/AEM.00662-17.

Muneer, F., Rasul, I., Azeem, F., Siddique, M.H., Zubair, M., Nadeem, H., 2020. Microbial polyhydroxyalkanoates (PHAs): efficient replacement of synthetic polymers. J. Polym. Environ. 28, 2301–2323. https://doi.org/10.1007/s10924-020-01772-1.

Nangle, S.N., Ziesack, M., Buckley, S., Trivedi, D., Loh, D.M., Nocera, D.G., Silver, P.A., 2020. Valorization of CO_2 through lithoautotrophic production of sustainable chemicals in Cupriavidus necator. bioRxiv. https://doi.org/10.1101/2020.02.08.940007, 2020.02.08.940007.

Orth, J.D., Thiele, I., Palsson, B.O., 2010. What is flux balance analysis? Nat. Biotechnol. https://doi.org/10.1038/nbt.1614.

Parlane, N.A., Gupta, S.K., Rubio-Reyes, P., Chen, S., Gonzalez-Miro, M., Wedlock, D.N., Rehm, B.H.A., 2017. Self-assembled protein-coated polyhydroxyalkanoate beads: properties and biomedical applications. ACS Biomater. Sci. Eng. https://doi.org/10.1021/acsbiomaterials.6b00355.

Pfeiffer, D., Jendrossek, D., 2012. Localization of poly(3-Hydroxybutyrate) (PHB) granule-associated proteins during PHB granule formation and identification of two new phasins, phap6 and phap7, in Ralstonia eutropha H16. J. Bacteriol. 194 https://doi.org/10.1128/JB.00779-12.

Pillai, A.B., Kumar, A.J., Kumarapillai, H., 2019. Synthetic biology and metabolic engineering approaches for improved production and recovery of bacterial polyhydroxyalkanoates. In: Next Generation Biomanufacturing Technologies, ACS Symposium Series. American Chemical Society, pp. 181–207. https://doi.org/10.1021/bk-2019-1329.ch009. SE–9.

Ponnusamy, V.K., Nguyen, D.D., Dharmaraja, J., Shobana, S., Banu, J.R., Saratale, R.G., Chang, S.W., Kumar, G., 2019. A review on lignin structure, pretreatments, fermentation reactions and biorefinery potential. Bioresour. Technol. 271, 462–472. https://doi.org/10.1016/j.biortech.2018.09.070.

Pötter, M., Madkour, M.H., Mayer, F., Steinbüchel, A., 2002. Regulation of phasin expression and polyhydroxyalkanoate (PHA) granule formation in Ralstonia eutropha H16. Microbiology.

Pötter, M., Müller, H., Reinecke, F., Wieczorek, R., Fricke, F., Bowien, B., Friedrich, B., Steinbüchel, A., 2004. The complex structure of polyhydroxybutyrate (PHB) granules: four orthologous and paralogous phasins occur in Ralstonia eutropha. Microbiology. https://doi.org/10.1099/mic.0.26970-0.

Qi, Q., Steinbüchel, A., Rehm, B.H.A., 2000. In vitro synthesis of poly(3-hydroxydecanoate): purification and enzymatic characterization of type II polyhydroxyalkanoate synthases PhaC1 and PhaC2 from Pseudomonas aeruginosa. Appl. Microbiol. Biotechnol. 54 https://doi.org/10.1007/s002530000357.

Qian, E.W., 2013. Pretreatment and saccharification of lignocellulosic biomass. In: Research Approaches To Sustainable Biomass Systems. https://doi.org/10.1016/B978-0-12-404609-2.00007-6.

Raza, Z.A., Abid, S., Banat, I.M., 2018. Polyhydroxyalkanoates: characteristics, production, recent developments and applications. Int. Biodeterior. Biodegrad. https://doi.org/10.1016/j.ibiod.2017.10.001.

Sabbagh, F., Muhamad, I.I., 2017. Production of poly-hydroxyalkanoate as secondary metabolite with main focus on sustainable energy. Renew. Sustain. Energy Rev. https://doi.org/10.1016/j.rser.2016.11.012.

Sharma, P.K., Fu, J., Spicer, V., Krokhin, O.V., Cicek, N., Sparling, R., Levin, D.B., 2016. Global changes in the proteome of Cupriavidus necator H16 during poly-(3-hydroxybutyrate) synthesis from various biodiesel by-product substrates. Amb. Express 6. https://doi.org/10.1186/s13568-016-0206-z.

Steinbüchel, A., Lütke-Eversloh, T., 2003. Metabolic engineering and pathway construction for biotechnological production of relevant polyhydroxyalkanoates in microorganisms. Biochem. Eng. J. 16, 81–96. https://doi.org/10.1016/S1369-703X(03)00036-6.

Tu, Q., Yin, J., Fu, J., Herrmann, J., Li, Y., Yin, Y., Stewart, A.F., Müller, R., Zhang, Y., 2016. Room temperature electrocompetent bacterial cells improve DNA transformation and recombineering efficiency. Sci. Rep. 6, 24648 https://doi.org/10.1038/srep24648.

Ushimaru, K., Motoda, Y., Numata, K., Tsuge, T., 2014. Phasin proteins activate aeromonas caviae polyhydroxyalkanoate (PHA) synthase but not ralstonia eutropha PHA synthase. Appl. Environ. Microbiol. 80 https://doi.org/10.1128/AEM.04179-13.

Wahl, A., Schuth, N., Pfeiffer, D., Nussberger, S., Jendrossek, D., 2012. PHB granules are attached to the nucleoid via PhaM in Ralstonia eutropha. BMC Microbiol. 12, 262. https://doi.org/10.1186/1471-2180-12-262.